Notes on the Design Strategy for the LCLS-II FEL Personnel Protection Stoppers

LCLSII-TN-15-36

9/29/2015

J. Krzywinski, J.T. DeLor, Y. Feng, P.A. Montanez, E. Ortiz, M. Rowen
SLAC, Stanford, CA 94036 USA

Notes on the Design Strategy for the LCLS-II FEL Personnel Protection Stoppers

J. Krzywinski, J.T. DeLor, Y. Feng, P.A. Montanez, E. Ortiz, M. Rowen

1. Introduction

The X-ray beam properties of the LCLS-II high repetition rate Free-Electron Laser (FEL) present both conceptual and implementation challenges to developing insertable devices that will stop such a beam securely and reliably. Existing stopper designs currently deployed on LCLS-I operating at a repetition rate of only 120 Hz will not work for LCLS-II which produces similar single pulse energies but with a maximum repetition rate up to 1 MHz; a nearly 4 orders of magnitude increase. The unique combination of the extremely high peak fluence and the enormous average power density, unprecedented at the existing 3rd generation synchrotron or the current 4th generation low repetition rate FEL sources, requires new solutions.

In this note we explore some of the possible solutions that can push the limits of the allowable average and peak power beyond what were considered up until now. As a starting point we set the requirement that the stopper should be able to stop/absorb a beam with an average power of up to 200 W and maximum credible single pulse energy from 2 mJ to 10 mJ [1]. The specific beam parameters considered were: 100 kHz, 2 mJ and 20-50 fs long pulses over the X-ray energy range of 0.2 to 5 keV (average power 200 W). The authors have not identified a solution for stopping a beam at a KW level average power coupled with an MHz repetition rate at the writing of this paper.

The combination of enormous average incident power density (W/cm^2) and extremely high peak fluence (J/cm^2 per pulse) suggests that the ideal material for stopping such X-ray beams should have both high thermal conductivity and low *Z* number; a low *Z* material is needed to avoid instantaneous damage. While there are several materials that can be considered, the most compelling low *Z* material is CVD diamond that possesses exceptional thermal conductivity. There is a potential risk that diamond has not been tested with respect to the instantaneous damage limit (usually specified in eV/atom), especially under high repetition conditions when other factors such as the cyclical thermal fatigue, phase transitions, and chemical stability are considered. A further challenge is the operation at or near the carbon *K*-edge where the X-ray absorption increases dramatically. Potentially the instantaneous damage problem can be mitigated by coating the CVD diamond by a thin layer of a damage resistant low *Z* material such as B_4C. The results of this study are described in section 2.

We have also investigated the possibility of using B_4C-based stoppers at grazing incidence. The LCLS-I experience has proven that B_4C-based stoppers can effectively handle the instantaneous damage problem, but B_4C's relatively poor thermal conductivity (~ 30 W/m-K at room temperature) raises a serious question of whether or not such a material can be used as stoppers for beams with high power densities. We have thus explored solutions using grazing incidence conditions where the power is spread over sufficiently larger areas. Grazing incidence copper-based stoppers have been

successfully used at 3rd generation X-ray sources to stop many kilowatt synchrotron X-ray beams, and grazing incidence B_4C based stoppers are also being planned to be used at the European X-ray FEL facility. We sought to answer the question of how the maximum allowable average power density depends on the angle of incidence. The results of this study are presented in section 3.

The conclusion of these works along with certain comparisons is presented in section 4.

2. CVD diamond based stoppers

CVD diamond has excellent thermal conductivity, almost two orders of magnitude higher than that of B_4C at room temperature and above. Therefore, one could expect that it should work at normal incidence.

We have considered two cases, which correspond to the maximum photon energy of 1300 eV for the Soft X-ray (SXR) and 5000 eV for the hard X-ray (HXR) beamlines, respectively. The X-ray FEL beam sizes at the worst-case scenarios at the stopper locations in the Front End Enclosure (FEE) (without the use of focusing lenses or mirrors) and the X-ray attenuation lengths at these two energies are given in Table 1. The thermal conductivity of CVD diamond assumed in simulations is shown in Fig. 1.

Photon energy [eV]	FWHM Beam size [μm]	Attenuation length [μm]
1300	1160	2.7
5000	322	150

Table 1: The X-ray FEL FWHM beam size and the X-ray attenuation length for CVD diamond at 1300 eV and 5000 eV.

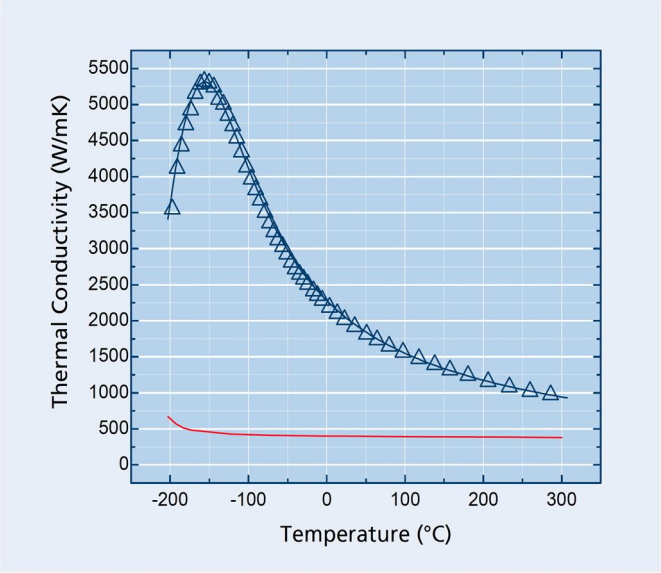

Fig. 1: The thermal conductivity of CVD diamond (blue line) and copper (red line) for comparison [data taken from Diamond Materials GmbH].

The simulations were performed using the finite element analysis (FEA) method. The average power was applied as if it were a CW source, and the pulse structure of the FEL beam was not considered for simplicity. The instantaneous temperature in the material is expected to oscillate around that obtained using the CW FEA analysis, and depends on the exact temporal structure of the pulses. In addition, the FEA calculations were crosschecked with the help of several finite difference algorithms to assure that there are no significant numerical errors due to the fact that the absorption length was much smaller than the dimensions of the stopper. The finite difference algorithms assumed constant thermal conductivity and crosschecks were performed at low power levels resulting in small temperature variations. We started our simulations with an edge-cooled model (fixed temperature). The geometry is depicted in Fig. 2.

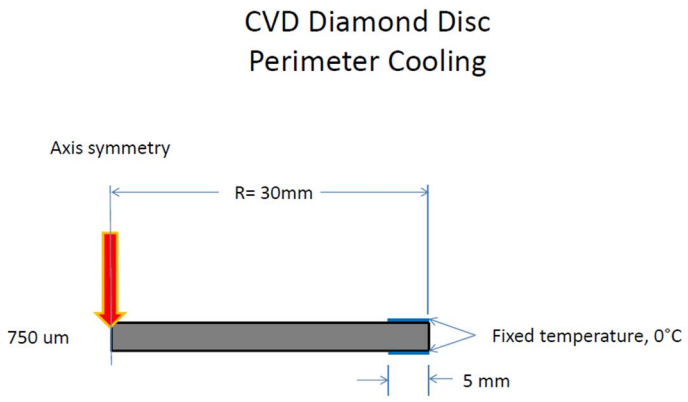

Fig. 2: The schematic of a perimeter cooled CVD diamond used in simulations. The FEL beam is incident normal to the top surface and at the center of a 750 μm thick diamond disk of 30 mm in radius with the edge being held to a fixed temperature of 0°C.

The dependence of the simulated maximum temperature as a function of the average incidence power for the 1300 eV case and the 5 keV case is illustrated in Fig. 3. For the SXR 1300 eV simulation, the energy absorbed in the material was assumed to be applied to the surface due to the very short absorption length of < 3 μm, whereas in the 5 keV HXR case, a volumetric heating model was used. As expected the maximum temperature in the diamond for the two cases stays in a safe region well below the graphitization temperature for diamond (1300 °C) at power levels up to 200 W.

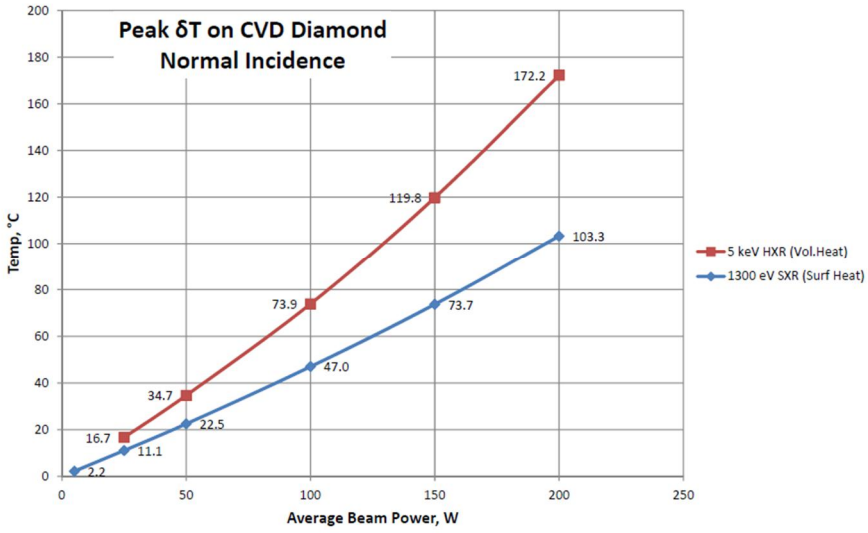

Fig. 3: The steady state maximum temperature in the diamond for the 1300 eV SXR and 5 keV HXR cases as a function of the (CW) incident power for the geometry shown in Fig. 2.

We have also simulated the thermal stress arising from the temperature gradient in the diamond. The boundary conditions are shown in Fig. 4. Here we used the most conservative conditions where cooled edges were bound. The stress distributions for the 5 keV/200 W cases are given in Fig. 5 and Fig. 6. The maximum stress is more than one order of magnitude smaller than the tensile strength of 500 MPa, at which the material is likely to be mechanically damaged. Therefore we have concluded that perimeter cooled CVD discs should be able to withstand the maximum average input power of 200 W. In addition, the stress analysis of the CVD diamond disc with the bounded edges leads to the conclusion that one can use indium foil as the thermal contact material between the diamond and a cooper cooling block.

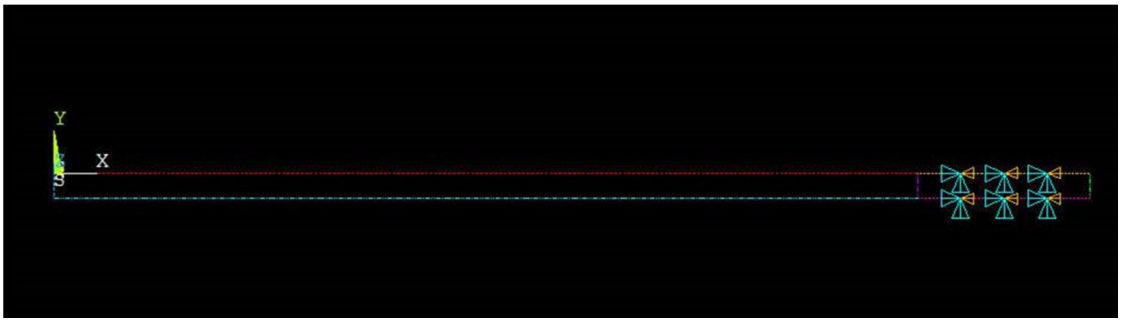

Fig. 4: The Boundary conditions with clamped edges (5mm edge restricted from movement in X and Y directions).

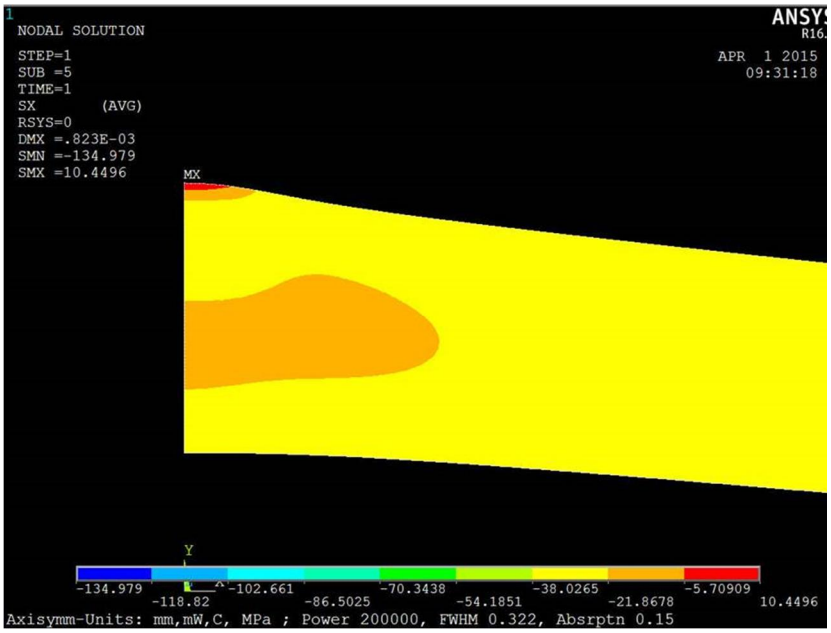

Fig. 5: Radial stresses. Extreme values: 10.45 MPa (tensile), -38 MPa (compressive)

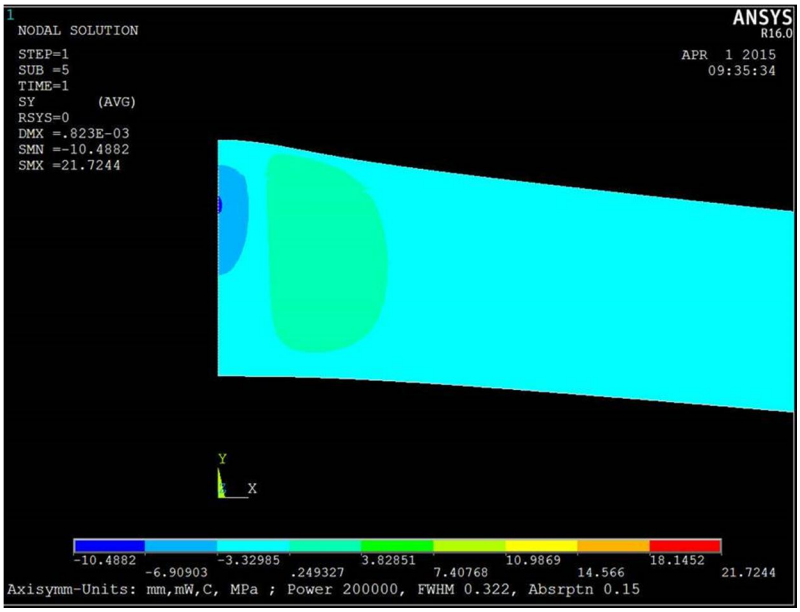

Fig. 6: Axial stresses. Extreme values: 7.4 MPa (tensile), -10.5 MPa (compressive)

The instantaneous damage problem has been studied extensively both theoretically and experimentally at LCLS-I and other FEL facilities [e.g. 2, 3]. The instantaneous damage happens on a time scale ranging from a few femtoseconds to tens of picoseconds. The energy of femtosecond photon pulses is first absorbed in the atom's electron system, which then thermalizes with the lattice on the time scale of 1 to 50 ps [4]. When the absorbed dose is higher than the heat of fusion (or a specific heat related to other phase transitions), melting and subsequent damages occur. The typical heat of fusion scale is on the order of 1 eV/atom. Both thermal and non-thermal damage mechanisms have been reported in the literature [3,6]. In the case of CVD diamond both the theory and the experiment support the non-thermal induced damage mechanism with a threshold around 0.5 eV/atom [6,7].

Fatigue related damages should also be considered in addition to the instantaneous damage [7]. The theory predicts that the fatigue related damage could occur if the instantaneous absorbed dose is larger than a certain fraction of the heat of fusion. However, the current theory [7] is directly applicable to ductile materials such as Be or Al. It is not clear how the same theory can be extended to other materials in which the yield strength is anisotropic. For example, in the case of B_4C no multi-shot damage was observed when the B_4C sample was exposed to 650,000 X-ray pulses depositing 0.16 eV/atom at the surface of the sample (the heat of fusion for B_4C is close to 0.5 eV/atom). The dose of 0.16 eV/atom is more than twice as high as the dose derived if one applies the lowest value of the yield strength, the tensile yield strength, to estimate the fatigue related damage for B_4C [8]. The reason that the experimentally determined fatigue threshold is at least twice higher than derived from the theory presented in [7] can be attributed to the fact that the thermal stress here has mainly a compressive component and that the compressive yield strength in B_4C is much higher than the tensile one. One can expect that a similar situation may occur in the case of CVD diamond.

The instantaneous damage problem is most severe at the lowest photon energies as the absorption coefficient increases with the third power of the wavelength. For the CVD diamond the maximum absorption occurs at the photon energy close to 290 eV which corresponds to the carbon K absorption edge. Taking into account expected LCLS-II beam parameters and the location of the stopper; one derives the peak dose of 0.1 eV/atom at this photon energy. We have calculated the maximum increase of the temperature ΔT at the surface by taking into account the nonlinear dependence of the specific heat. The expected peak dose of 0.1 eV/atom corresponds to a ΔT of about 700 ^{o}K. The peak dose of 0.1 eV/atom has the same order of magnitude as the safe limit for the multi-shot damage. Therefore, in order to mitigate the multi-shot damage risk, we propose to coat the CVD surface with thin layer (1-2 μm) of B_4C. The effect of the coating on the peak dose absorbed in CVD diamond is shown in Fig. 7. We are also planning to perform multi-shot damage tests to mitigate the thermal fatigue risk even further.

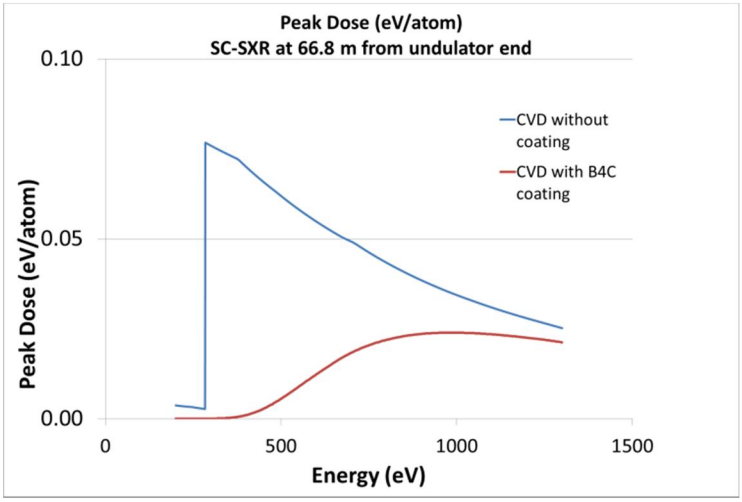

Fig. 7: The Peak dose of coated (red line) and uncoated CVD diamond (blue line).

The B_4C coated CVD diamond discs with the perimeter cooling will be placed in front of other stopper's elements fabricated from SiC and tungsten and designed to stop higher photon energies (see Fig. 8). The role the diamond discs is twofold: 1) to dissipate the heat and to reduce the thermal load on SiC parts from 200 W to less than 2 W between 200 eV and 5000 eV, and 2) to protect SiC block from instantaneous damage in the same photon range. For photon energies higher than 5 keV up to 25 keV, the stopper will be working at the 120 Hz pulse frequency with the average power on the order of few Watts. The SiC block will protect the tungsten (for bremsstrahlung attenuation purpose) and other metals from instantaneous damage at photon energies higher than 5 keV. The dimensions of the SiC and tungsten blocks will be optimized later.

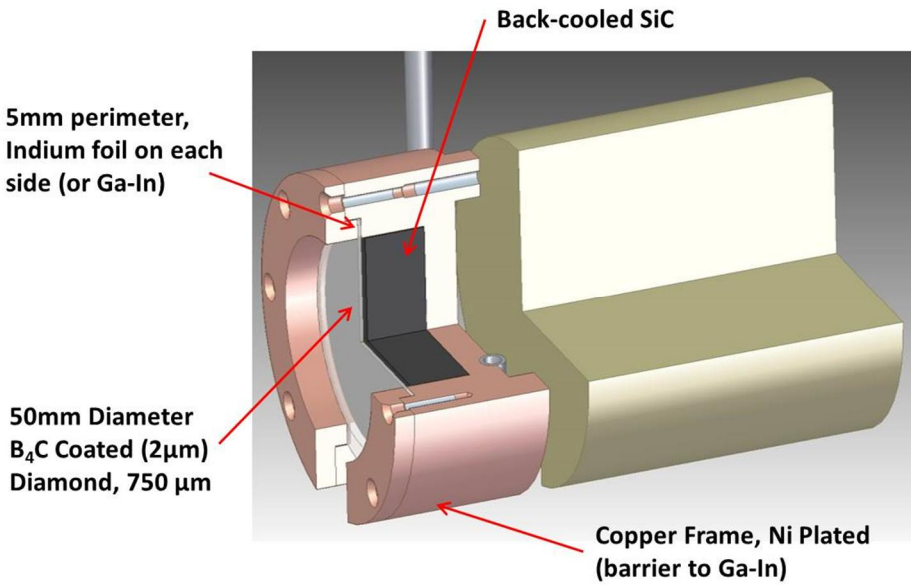

Fig. 8: A 3D rendering of the CVD stopper (active burn-through monitor not shown)

3. B_4C based stopper

In this section we consider only the average power for a B_4C based stopper. The instantaneous damage issues are well understood and have been investigated experimentally at LCLS I.

Grazing incidence, copper based stoppers have been successfully used at 3rd generation x-ray sources to stop kilowatt synchrotron radiation beams. Grazing incidence B_4C based stoppers are planned to be used at European X-FEL [9].

The idea of managing the temperature by spreading the average power over larger areas works well when the absorption length is much smaller than the beam size. In the opposite case a pencil like beam generates most of the heat inside the volume of a stopper and changing the angle of incidence is not very effective with respect to the diminishing of surface temperature.

In order to address this problem we have investigated a model of the stopper which consists of a 6 mm thick B_4C material which is brazed to a molybdenum block (compatible CTE for brazing) and is cooled at the back side such that its temperature is kept at zero °C. The geometry and boundary conditions (for the normal incidence case) are presented in Fig. 9.

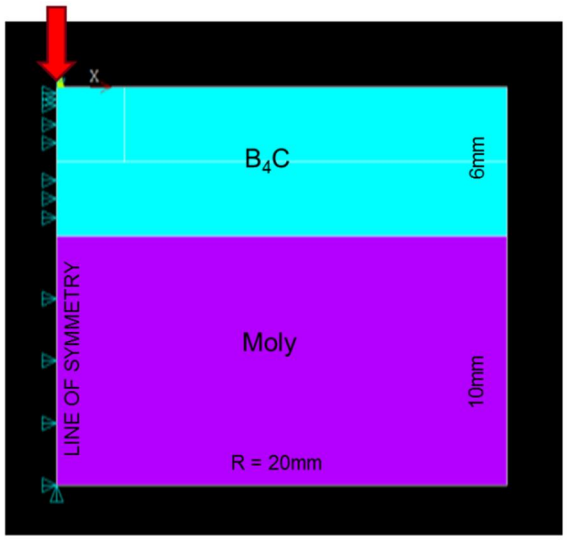

Fig. 9: The geometry and boundary conditions of the B_4C stopper model at normal incidence

We have considered two cases which correspond to the maximum photon energy of 1300 eV and 5000 eV for the SXR and HXR beam lines respectively. The beam sizes and attenuation lengths are presented in the Table 2. The thermal conductivity of B_4C assumed in simulations is shown in Fig. 10

Photon energy [eV]	FWHM Beam size [microns]	Attenuation length [microns]
1300	1160	6
5000	322	351

Table 2: FWHM beam sizes and attenuation lengths for B_4C at 1300 eV and 5000 eV

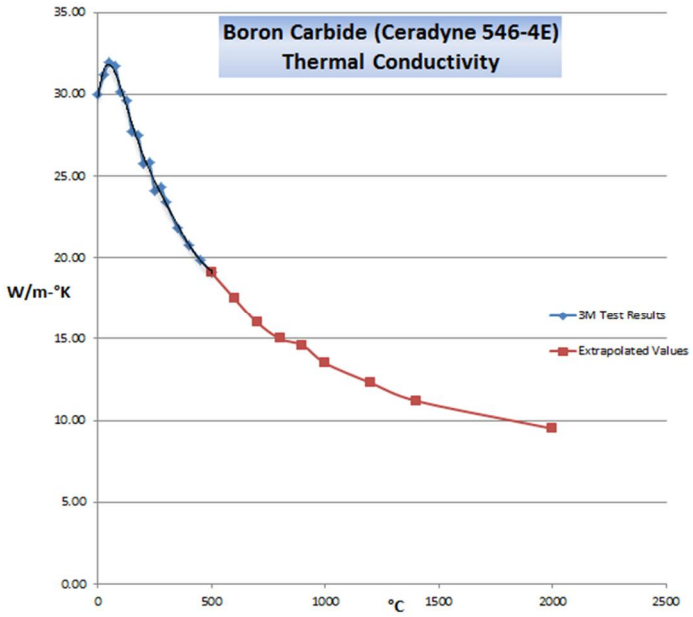

Fig. 10: Dependence of thermal conductivity on temperture

The low absorption coefficient of B_4C (which is necessary to mitigate the instantaneous damage problem) results in a large absorption length. For example, at the photon energy of 5 keV, the absorption length is in the same order as the beam size. Therefore one should study in more detail how the spreading of the average power works in the case of B_4C based stoppers at this photon energy. For the normal incidence condition the steady state surface temperature of the stopper reaches the melting temperature for the incidence power in the order of 50 W. The distribution of the stopper's temperature is presented in Fig. 11a.

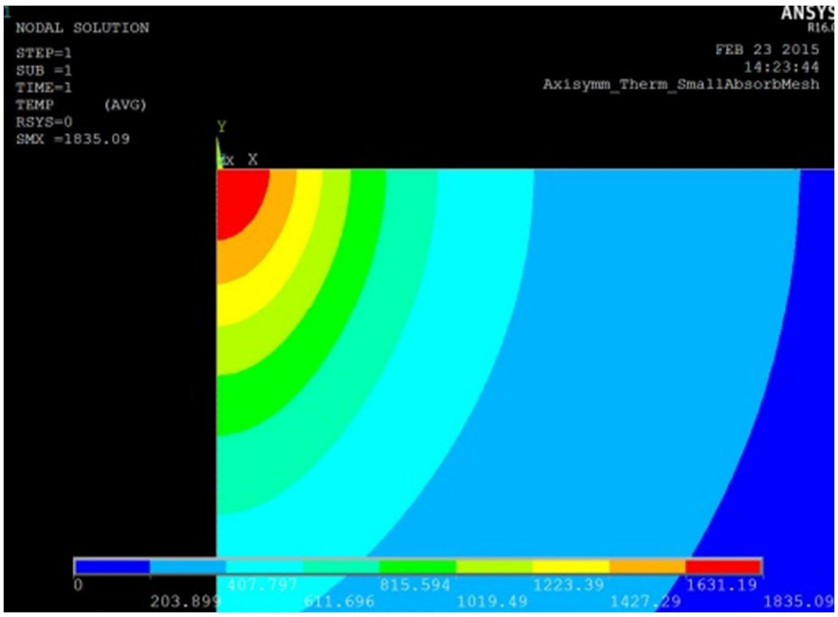

Fig. 11a: Temperature distributon

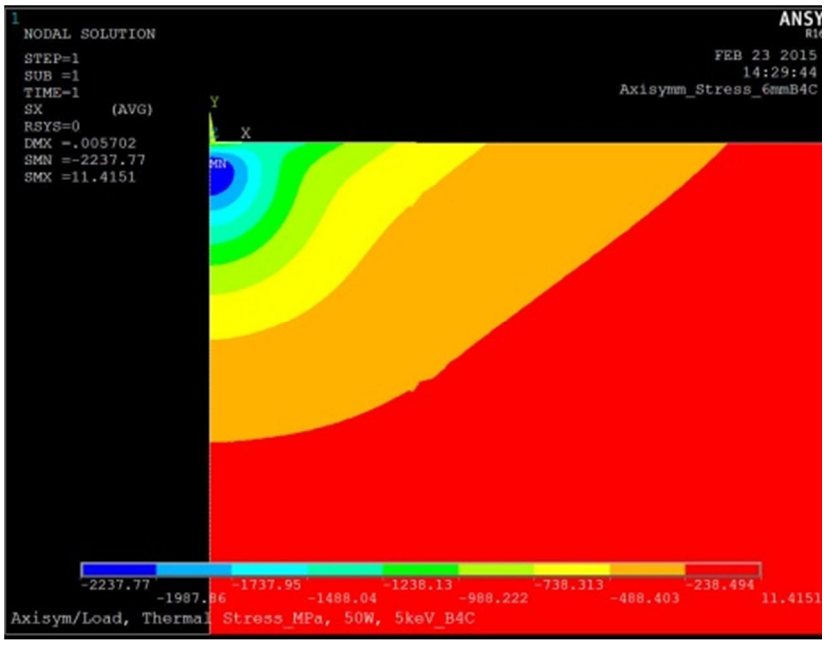

Fig. 11b: Radial Stress distributon

The stress distribution is presented in Fig. 11b. The thermal stress has mainly the compressive component. The tensile stress is much lower and it is approximately one order of magnitude smaller than the tensile strength which is in order of 500 Mpa. The main conclusion form this result is that the temperature damage will precede the stress related damage.

The dependence of the incidence angle on the temperature of the stopper's surface is discussed next. The summary of simulations is presented in Fig. 12. In this figure we plot the dependence between the incidence average power and the incidence angle which results in the same temperature at the surface. We plot three dependencies which correspond to the increase of temperature at the surface by 1000 °K, 1500 °K and up to near the melting temperature of 2445 °C.

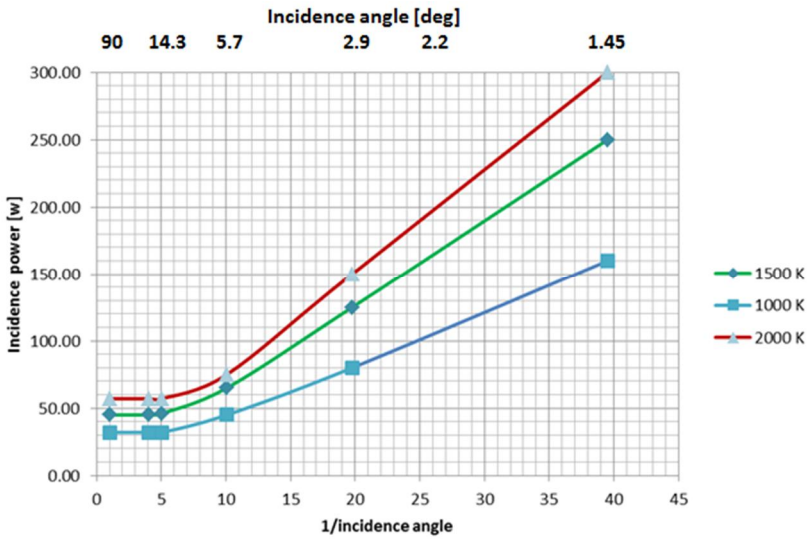

Fig.12: Dependence between angle of incidence and incident power for constant surface temperature

One can clearly see from the figure that spreading the area of the illumination at the surface by the factor up to 10 times is not very effective. It increases the tolerable incidence power only up to 1.5 times. In order to gain an increase in the power by more than 3 times it is necessary to decrease the incidence angle below 3 degrees.

It can also be seen in this figure that in order to stay 400 °K below the melting temperature at the incidence power of 200 W the angle of incidence should be smaller than 2.2 degrees. Such a shallow angle will largely increase the longitudinal dimension of a stopper, which in turn will occupy more of the limited, valuable space of the diagnostics area. This would also increase the volume and the cost of B_4C material.

Unfortunately, at the time of publishing we don't have FEA simulations results for the temperature dependence on the grazing incidence for the 1300 eV case. However, based on the finite difference simulations and using interpolations in order to take into account nonlinear character of the thermal conductivity, we have concluded that to stay below 2000 °C at the incidence power of 200 W, the angle of incidence should be smaller than 9 degrees. For the same power the angle of incidence should be smaller than 5 degree in order to keep the surface temperature below 1000 °C.

4. Discussion and conclusions

In this section we will discuss feasibility of building the LCLS-II stoppers according to the two approaches discussed above. We will estimate the physical dimensions, and consider engineering efforts and costs. Then we will debate on other aspects such as risk, and going beyond the initial requirements, keeping in mind possible further developments of LCLS-II which can result in increasing the photon energy range and the instantaneous power and the average power.

The considerations presented in the previous sections suggest that two concepts could be realized in practice.

4.1 CVD based stopper

The normal incidence geometry allows designing very compact stoppers. Two redundant stoppers should use only around 300 mm space of the XTES beamline. Miniaturization of XTES elements has a great value because it gives a room for more diagnostics, which can be needed as the development of the LCLS-II machine progresses.

Temperature and stress analysis suggests that CVD based stopper should endure twice or more of the design target average power of 200 W at 5 keV photon energy. B_4C coated CVD diamond should also survive higher pulse energies than specified in the PRD document. This prediction is based on the measured radiation hardness B_4C and the fact that both materials have similar compressive and tensile yield strength. However, the issue of resistance of CVD to instantaneous doses has not been explored yet experimentally and needs to be tested.

Here the main concern is that CVD diamond has a phase transition to graphite at the temperature around 1300 °C. Therefore the surface temperature should always be kept below this value and the stresses reevaluated with each increase. The limits of the performance of the CVD based stopper with respect to the average power and the maximum pulse energy should be evaluated experimentally.

The FEA simulations should be revisited when the actual values for conductance are known at the cooling boundaries. This will result in an increase of the steady state peak temperatures deltas from the “fixed temperature” scenario assumed above. Initial studies indicate this might be on the order of a 50% increase in peak temperature delta for CVD, but still only a fraction of the graphitization temperature.

The significant advantage of CVD based stopper is that it has basically the same design for both SXR and HXR beam lines and this significantly reduces engineering efforts and promotes commonality between beamline devices; an operational benefit.

4.2 B4C based stopper

The cost analysis of the B_4C based stopper suggests that material cost should be similar to the CVD based stopper. The length of two redundant stoppers is estimated to be around 800 mm (9 degrees grazing incidence) and 1500 mm (2.2 degrees grazing incidence) for the SXR and HXR cases respectively. Because SXR and HXR stoppers are different, an additional engineering cost is required here. This additional cost offsets the cost of tests required to determine radiation hardness of B_4C coated CVD diamond.

The performance of B_4C stoppers barely meets the design target of 200 W of average power at the discussed grazing angle. While there is still possible to increase the tolerable average power for the SXR stoppers, by decreasing the angle of incidence, there is no much room for improvements for the HXR stopper. 400 W of acceptable average power will require changing the grazing incidence angle to 1.07 degrees and increasing the length of the stopper to 3 meters which is unpractical.

5. Conclusions

In summary we have shown that CVD based concept of the LCLS-II stopper is better and more practical with respect to B_4C based stopper. While the cost of realization of two concepts that could endure average power of 200 W is similar, the CVD based concept has two main advantages:

1. CVD Diamond handles higher average power and power density than B_4C stopper.
2. CVD Diamond occupies significantly less beamline space in XTES than the B_4C stopper.

The radiation hardness of CVD diamond is less understood than the B_4C hardness, but the risk of radiation damage will be mitigated by coating CVD diamond with 1-2 micron thick B_4C layer. The limits of the performance of the CVD diamond based stopper with respect to the average power and the maximum pulse energy should be evaluated experimentally as a follow-up to this initial analysis.

We would like to thank L. Zhang for helpful discussions.

References:

1. X-ray Transport and Experimental Systems Physics Requirements document: LCLSII-3.5-PR-0051-R1
2. S. P. Hau-Riege et. al,, Optics Express **18**, 23933-23938 (2010).
3. S.P. Hau-Riege et. al., Appl. Phys. Lett. **95**,11104 (2009).
4. B. Ziaja, et. al., High Energy Density Phys. **9** (2013) 462-472
5. J. Gaudin, et. al, *Phys. Rev. B* **88** (2013) 060101
6. N. Medvedev, et. al., Phys. Rev. B **88**, (2013) 224304
7. D.D. Ryutov, Rev. Sci. Instr. **74**, 3722 (2003).
8. S.P. Hau-Riege, LCLS note, LCLS-TN-06-5 (2006)
9. H. Sinn, Personal communication